JOURNAL OF SPACECRAFT AND ROCKETS
Vol. 29, No. 5, September–October 1992

Steady and Quasisteady Resonant Lock-In of Finned Projectiles

N. Ananthkrishnan* and S. C. Raisinghani†
Indian Institute of Technology, Kanpur 208016, India

Equations of motion for a rolling finned projectile presented by an earlier investigator are corrected. Steady resonant lock-in solutions, both normal and reverse, are presented and their stability investigated. Two-dimensional topological models are constructed to explain how the occurrence of resonant lock-in depends on initial conditions. Results from numerical simulations are used to validate the suggested models. Quasisteady-state (QSS) resonant lock-in is shown to be possible for an unstable equilibrium solution at resonance. QSS solutions are found to lead to divergent yaw behavior typical of catastrophic yaw. It is suggested that catastrophic yaw can be demonstrated by modeling the effect of the nonlinear induced side forces and moments at resonance as a reduction in yaw damping.

Nomenclature

G = $-(\hat{r}_c h C_{N\alpha}/2)(C_{M0}/C_{M\alpha})[C_{lp} + (I_x/ml^2)C_D][-(1-\sigma)/M]^{1/2}$
$\hat{H}$ = $(\rho Sl/2m)[C_{L\alpha} - C_D - (ml^2/I)(C_{Mq} + C_{M\dot{\alpha}})] \times [-(1-\sigma)/M]^{1/2}$
h = $(\hat{H} - \sigma\hat{T})/(1-\sigma)$
I = transverse moment of inertia
I_x = axial moment of inertia
$\hat{K}_p$ = $-(\rho Sl^3/2I_x)[C_{lp} + (I_x/ml^2)C_D][-(1-\sigma)/M]^{1/2}$
l = reference length, diam
M = $(\rho Sl^3/2I)C_{M\alpha}$
m = mass
$\hat{r}_c$ = radial center of mass offset, calibers
S = reference area
$\hat{T}$ = $(\rho Sl/2m)[C_{L\alpha} + (ml^2/I_x)C_{Mp\alpha}][-(1-\sigma)/M]^{1/2}$
t = time
t_1 = $[-M/(1-\sigma)]^{1/2}\int_0^t (V/l)\,dt$
$y, \dot{y}$ = displacement and velocity variables used for two-dimensional topological models
δ = absolute value of $\tilde{\tau}$
$\tilde{\theta}$ = orientation angle of $\tilde{\tau}$
ρ = air density
σ = I_x/I
μ = $-(C_{M\alpha}/C_{M0})h\tilde{\tau}e^{-i\theta}$
$\tilde{\tau}$ = total incidence angle, $= \tilde{\beta} + i\tilde{\alpha} = -\delta e^{-i\tilde{\theta}}$
ϕ = roll angle
ϕ_M = asymmetry moment orientation angle

Subscripts

e = equilibrium value
s = steady-state value

Superscripts

$\bar{}$ = complex conjugate
$\dot{}$ = $d(\,)/dt_1$

Received May 7, 1991; revision received March 27, 1992; accepted for publication April 8, 1992.

*Graduate Student, Aerospace Engineering Department; currently Doctoral Student, Aerospace Engineering Department, Indian Institute of Technology, Powai, Bombay 400076, India.
†Professor, Aerospace Engineering Department.

Introduction

ROLL resonance occurs when the roll rate of a finned projectile matches its natural yawing frequency. A projectile with slight configuration asymmetry has equal natural frequency in pitch and yaw but has a nonzero trim angle. At resonance, this trim angle gets magnified, leading to large-amplitude oscillations. Since projectiles are usually designed to have marginal static stability, small rolling moments produced in flight could easily push the projectile into roll resonance.

This can be avoided by canting the fins and rolling the projectile through the resonance region to a desired steady-state roll rate. Linear aeroballistic theory[1] predicts that the projectile will roll through the resonance value of roll rate and only a fraction of the resonant trim magnitude would be observed. On the contrary, many projectiles were seen[2] to get locked in at resonance with even larger amplitudes of oscillation than predicted by the linear theory. This phenomenon of roll lock-in has been attributed to nonlinear roll moments induced by the trim angle.[3] It has been suggested[4] that an offset center of mass is the primary cause of these induced roll moments. The phenomenon of roll lock-in and other anomalous roll behavior of finned projectiles like catastrophic yaw and transient resonance have been discussed by Barbera[5] and Murphy.[6]

A recent publication by Murphy[7] has approached the problem of roll lock-in analytically. However, the pitch-yaw equation reported in Ref. 7 [Eq. (22)] is incorrect. In this paper, we present revised numerical results for equilibrium solutions and their stability with the corrected equation. We then seek to expand on the existing work. Two-dimensional topological models are put forward to explain how occurrence of resonant lock-in solutions depends on initial conditions. We propose to show that an unstable equilibrium at resonance may lead to quasisteady lock-in. Finally, we take a look at the phenomenon of catastrophic yaw.

Equilibrium Solutions

The equations of motion are written in an aeroballistic axis system. This is illustrated in Fig. 1, which is, in part, adapted from Ref. 8. The positive sense for the angles of attack and sideslip is indicated in the figure. With the complex angle of attack (total incidence angle) as defined in Fig. 1, the pitch-yaw equation can be written as

$$\ddot{\mu} + [\hat{H} + i(2-\sigma)\dot{\phi}]\dot{\mu} + [(1-\sigma)(1-\dot{\phi}^2 + i\dot{\phi}h) + i\dot{\phi}]\mu = -(1-\sigma)h\exp(i\phi_M) \quad (1)$$

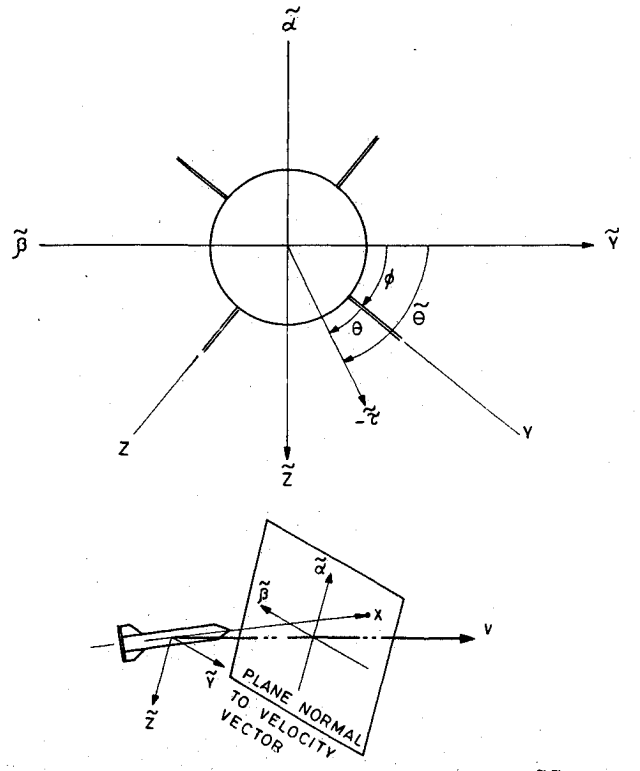

Fig. 1 Complex angle of attack: YZ—missile-fixed axes, $\tilde{Y}\tilde{Z}$—aeroballistic axes.

It was pointed out by Murphy during the review process that the term $(1-\sigma)$ multiplies only the first three terms in the coefficient of μ and not the $i\dot{\phi}$ term as reported in Eq. (22) of Ref. 7.

The roll equation for a projectile with an induced rolling moment due to an offset center of mass [i.e., $n=1$ in Eq. (19) of Ref. 7] is

$$\ddot{\phi} + \hat{K}_p[\dot{\phi} - \dot{\phi}_s - iG(\mu - \bar{\mu})] = 0 \tag{2}$$

Equilibrium solutions of this system of equations [Eqs. (1) and (2)] are obtained from

$$f = \dot{\phi}_e - \dot{\phi}_s - iG(\mu_e - \bar{\mu}_e) = 0 \tag{3}$$

$$\mu_e = -h(1 - \dot{\phi}_e^2 + i\dot{\phi}_e h)^{-1} \exp(i\phi_M) \tag{4}$$

In the preceding equations, h is the aerodynamic asymmetry with orientation ϕ_M and G the magnitude of the center-of-mass offset.

Stability Analysis

We make use of Lyapunov's first method to investigate the stability of the equilibrium solutions of Eqs. (1) and (2). Following Ref. 7, we assume a small perturbation of an equilibrium state:

$$\dot{\phi} = \dot{\phi}_e + d_1 \tag{5a}$$

$$\mu = \mu_e + d_2 + id_3 \tag{5b}$$

$$\dot{d}_2 = d_4 \tag{5c}$$

$$\dot{d}_3 = d_5 \tag{5d}$$

Equations (1) and (2) can be cast as a system of five first-order differential equations,

$$\dot{x} = f(x;\ \dot{\phi}_s,\ h,\ \phi_M,\ G) \tag{6}$$

Using the small perturbation terms defined by Eq. (5), Eq. (6) can be written for a given set of parameters as

$$\dot{d} = Ad + g(d) \tag{7}$$

where $g(d)$ represents higher order terms that can be neglected in the linear approximation. The elements of the 5×5 matrix A, called the stability matrix, are listed in Table 1. The condition for stability requires all of the eigenvalues of matrix A to have negative real parts.

We choose $h = 0.1$, $\dot{\phi}_s = 3.0$, and $G = 5.0$. Equilibrium solutions, given by the roots of Eq. (3), for $\phi_M = 90$ and 270 deg, are listed in Tables 2 and 3, respectively. Eigenvalues of the A matrix corresponding to these equilibrium solutions are also given in Tables 2 and 3 for $\hat{H} = 0.1$, $\hat{K}_p = 0.1$, and $\sigma = 0.1$. The tables show that, for a stable equilibrium solution at resonance, normal ($\dot{\phi}_e \approx 1.0$), or reverse ($\dot{\phi}_e \approx -1.0$), there exists an unstable solution whose equilibrium roll rate is very near that of the stable resonance solution. This is seen[9] to be true for a wide range of parameters h, ϕ_M, and G.

Effect of Initial Conditions

In nonlinear systems with more than one equilibrium point, the steady-state solution depends on the initial condition. Tables 2 and 3 each show two stable equilibrium points—a design solution and a resonance solution. It is of interest to know, for a realistic set of initial conditions, which of these equilibrium solutions is attained in the steady state. In other words, one wishes to estimate the probability of occurrence of a resonant lock-in solution.

Qualitative Approach

We construct two-dimensional topological models to explain the behavior of trajectories originating from different initial points. In two dimensions, a stable (unstable) solution is represented by a stable (unstable) focus and a divergent solution by a saddle. The model corresponding to solutions C, D, and E of Table 2 is pictured in Fig. 2. Solutions A and B are not included in the model as they are well separated from the other three solutions. Examples of trajectories leading to lock-

Table 1 Stability matrix elements

$A_{11} = -\hat{K}_p$	$A_{12} = 0$	$A_{13} = -2G\hat{K}_p$	$A_{14} = 0$	$A_{15} = 0$
$A_{21} = 0$	$A_{22} = 0$	$A_{23} = 0$	$A_{24} = 1$	$A_{25} = 0$
$A_{31} = 0$	$A_{32} = 0$	$A_{33} = 0$	$A_{34} = 0$	$A_{35} = 1$
$A_{41} = [2\dot{\phi}_e \operatorname{Re}(\mu_e) + h \operatorname{Im}(\mu_e)](1-\sigma) - \hat{K}_p \operatorname{Im}(\mu_e)$				
$A_{42} = -(1-\sigma)(1-\dot{\phi}_e^2)$		$A_{43} = (1-\sigma)h\dot{\phi}_e - 2\hat{K}_pG \operatorname{Im}(\mu_e)$		
$A_{44} = -\hat{H}$		$A_{45} = (2-\sigma)\dot{\phi}_e$		
$A_{51} = [2\dot{\phi}_e \operatorname{Im}(\mu_e) - h \operatorname{Re}(\mu_e)](1-\sigma) + \hat{K}_p \operatorname{Re}(\mu_e)$				
$A_{52} = -(1-\sigma)h\dot{\phi}_e$		$A_{53} = -(1-\sigma)(1-\dot{\phi}_e^2) + 2\hat{K}pG \operatorname{Re}(\mu_e)$		
$A_{54} = -(2-\sigma)\dot{\phi}_e$		$A_{55} = -\hat{H}$		

Table 2 Equilibrium solutions for $\phi_M = 90$ deg

Case	$\dot{\phi}_e$	μ_e	Eigenvalues	Stability
A	−1.086	0.247 + i0.408	−0.055 ± i1.982 −0.484, 0.483 −0.188	Unstable (Divergent)
B	−1.027	0.758 + i0.404	−0.052 ± i1.916 −0.933, 0.770 −0.032	Unstable (Divergent)
C	1.011	−0.944 + i0.205	−0.050 ± i1.926 −0.078 ± i0.938 −0.045	Stable
D	1.241	−0.040 + i0.176	−0.051 ± i2.129 −0.197 ± i0.376 0.195	Unstable (Divergent)
E	2.861	−0.001 + i0.014	−0.056 ± i3.676 −0.050 ± i1.760 −0.089	Stable

Table 3 Equilibrium solutions for $\phi_M = 270$ deg

Case	$\dot{\phi}_e$	μ_e	Eigenvalues	Stability
A	−0.976	$-0.829 + i0.403$	$-0.039 \pm i1.891$	Stable
			$-0.092 \pm i0.878$	
			−0.038	
B	−0.862	$-0.155 + i0.389$	$-0.038 \pm i1.771$	Unstable
			$-0.187 \pm i0.444$	(Divergent)
			0.150	
C	0.754	$0.039 + i0.225$	$-0.063 \pm i1.664$	Unstable
			$0.112 \pm i0.321$	(Oscillatory)
			−0.399	
D	0.990	$0.971 + i0.195$	$-0.059 \pm i1.878$	Unstable
			−1.033, 0.897	(Divergent)
			−0.046	
E	3.115	$0.0004 - i0.0115$	$-0.059 \pm i3.919$	Stable
			$-0.037 \pm i1.999$	
			−0.108	

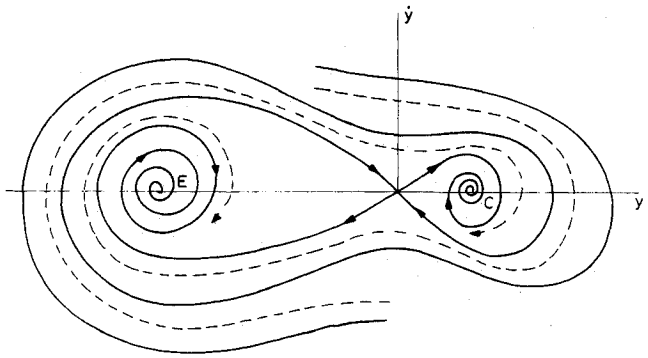

Fig. 2 Topological model for normal lock-in.

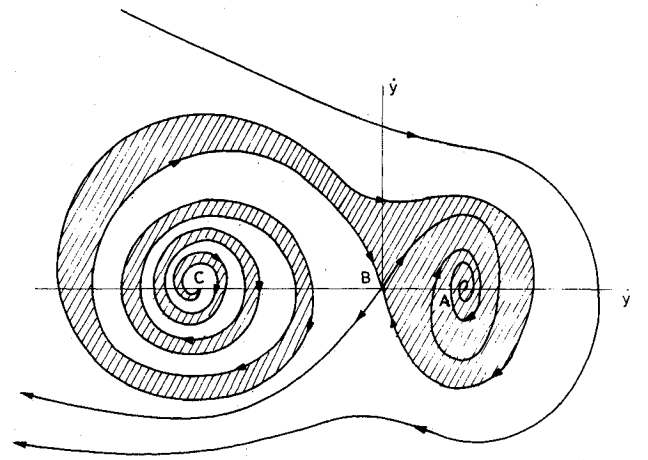

Fig. 3 Topological model for reverse lock-in.

in and to the design solution are also sketched in Fig. 2. It seems reasonable to conclude from Fig. 2 that a trajectory originating from an arbitrarily chosen initial condition is as likely to end up at C as at E.

The topological model for the reverse resonance case of Table 3, sketched in Fig. 3, looks different. The hatched area indicates all of the initial conditions that lead to lock-in. The other trajectories seen diverging to the left in Fig. 3 would eventually converge at the equilibrium point corresponding to the design solution (not shown in the figure). Figure 3 seems to suggest that reverse lock-in would be likely for only a very restricted set of initial conditions.

Numerical Simulation

We seek to validate the conclusions arrived at from the topological models by numerically integrating Eq. (6) for a number of initial conditions. Initial conditions arise as a result of disturbances in the process of firing a projectile and normally take the form of a yaw rate. Four values for the magnitude of the initial complex angular velocity were chosen, viz., 0.1, 0.2, 0.5, and 1.0. For each of these values, four orientation angles—0, 90, 180, and 270 deg—were used; that is, a total of 16 initial conditions were tested. Typical simulation responses for the roll rate and magnitude of the total incidence angle are shown in Figs. 4 and 5 for normal and reverse lock-in, respectively. The simulation studies showed that normal lock-in occurred for nearly half of the cases tested, whereas reverse lock-in was observed for only the odd case. This agrees very well with the qualitative picture given by the topological models.

Quasisteady-State Solutions

Stability of the equilibrium points listed in Tables 2 and 3 depends on the parameters $\hat{H}$, $\hat{K}_p$, and σ. Studies revealed that $\hat{H}$, which represents the damping in yaw, is found to be the most significant. Root locus plots for the eigenvalues corresponding to the resonance solution (case C) and the design solution (case E) of Table 2 are shown in Figs. 6 and 7, respectively. With decreasing values of $\hat{H}$, both of these solutions can be seen to become unstable. The other three unstable solutions of Table 2 are found to remain unstable for this range of values of $\hat{H}$.

It may be noted that for some values of $\hat{H}$, a pair of poles corresponding to the design solution has crossed over to the right half-plane while the resonance solution is still stable. Numerical simulation results for one such value of $\hat{H}$ (= 0.06) are shown in Figs. 8 and 9 over an extended time period. The roll rate can be observed to reach the design value where it shows oscillations of increasing amplitude. The total incidence angle builds up well beyond the resonant value for a body-

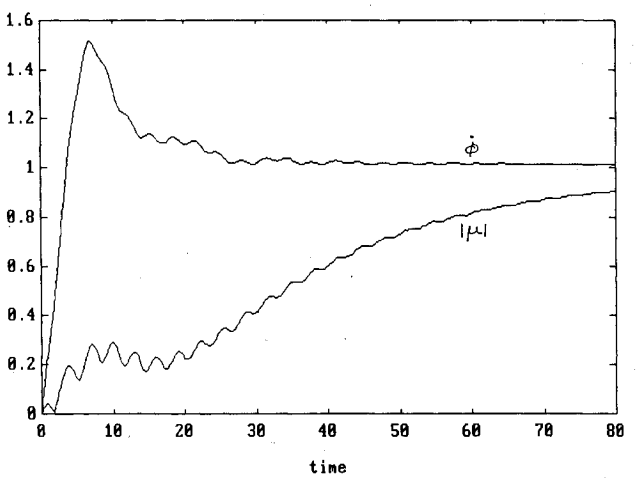

Fig. 4 Normal lock-in, case C of Table 2, for $\mu_0 = 0 + i0.1$.

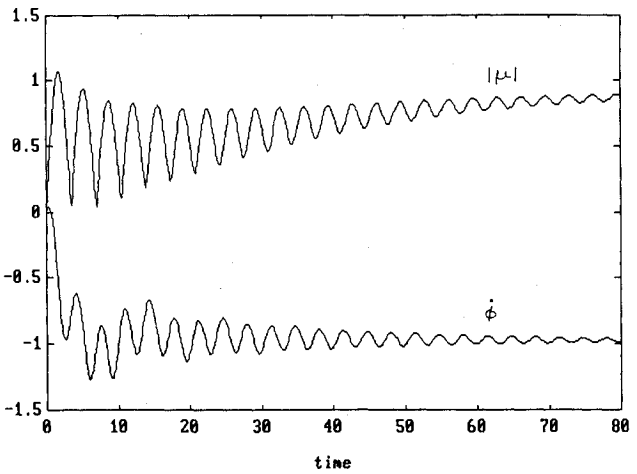

Fig. 5 Reverse lock-in, case A of Table 3, for $\mu_0 = 0 + i1.0$.

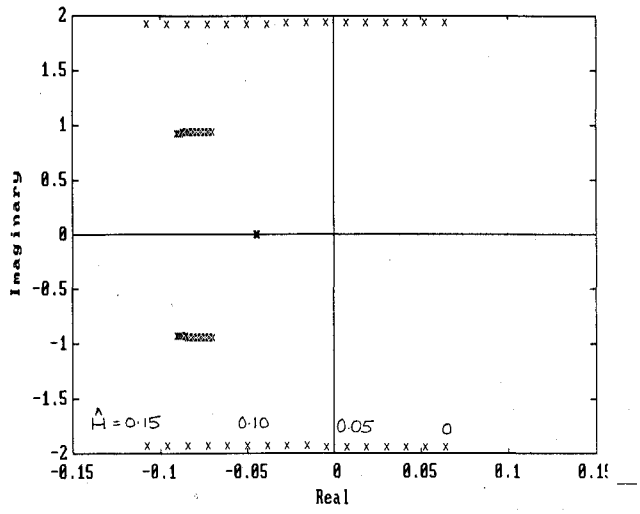

Fig. 6 Root locus for normal lock-in solution, case C of Table 2, with parameter $\hat{H}$.

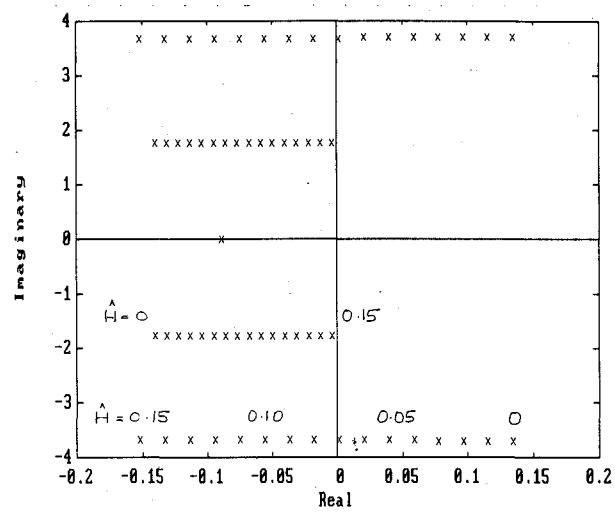

Fig. 7 Root locus for design solution, case E of Table 2, with parameter $\hat{H}$.

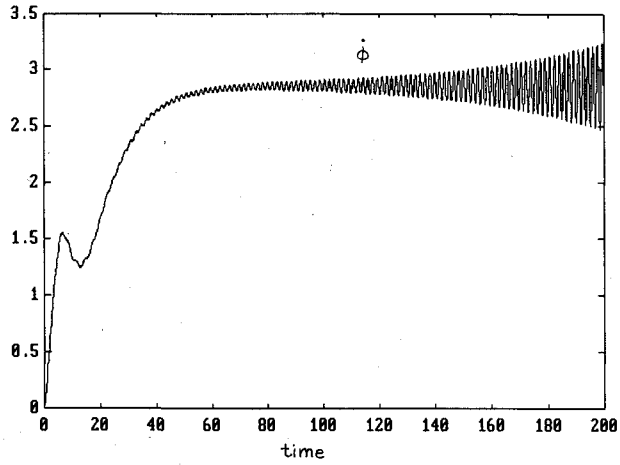

Fig. 8 Roll rate response for QSS solution ($\mu_0 = 0$).

fixed asymmetry and is seen to become unbounded. This corresponds to an outward spiraling motion in the $\tilde{\alpha}$-$\tilde{\beta}$ plane. Such a response is unexpected and shows that a divergence in yaw can occur despite the design value of roll rate being achieved.

The preceding analysis reveals a new and interesting result that an unstable equilibrium point as determined from small perturbation stability analyses can produce quasisteady-state (QSS) solutions. These solutions are labeled quasisteady since the variables do not attain constant steady-state values. Clearly, such solutions are of practical relevance for the missile designer. This also refutes the assertion made by Murphy[7] that unstable equilibrium solutions have no engineering significance. At the same time, it must be mentioned that the range of values of $\hat{H}$ for which QSS solutions can be expected for the parameters used in this paper is extremely limited. This can be seen from the root locus plots of Figs. 6 and 7. This may or may not be true for other combinations of the parameters and will require detailed investigation.

No simple two-dimensional topological model can be constructed for QSS solutions. A possible model to investigate the effect of initial conditions is shown in Fig. 10. The figure suggests that there exists a wide range of initial conditions for which QSS solutions may be expected. This is borne out by numerical simulation studies similar to those reported for steady lock-in solutions. However, no limit cycle motion as pictured in Fig. 10 could be observed about the unstable equilibrium point. To that extent, the model is approximate; but it serves the limited purpose of establishing how the attainment of QSS solutions depends on the initial conditions.

Catastrophic Yaw

Catastrophic yaw[3] is a dynamic instability experienced by projectiles locked in at resonance resulting in an unlimited build up of yaw. Nonlinear induced side forces and moments have been held responsible for this phenomenon. The effect of these additional forces is essentially to reduce the damping in yaw of the system. For some set of values of the parameters, different from that used in this study, one can expect that, with decreasing values of $\hat{H}$, the eigenvalues of the resonance solution (case C of Table 2) will become unstable before those of the design solution (case E). There would, therefore, exist a range of values of $\hat{H}$ for which the design solution would be

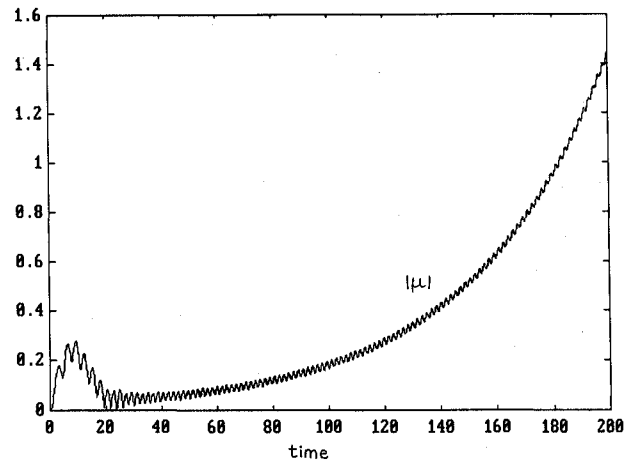

Fig. 9 Total incidence angle response for QSS solution ($\mu_0 = 0$).

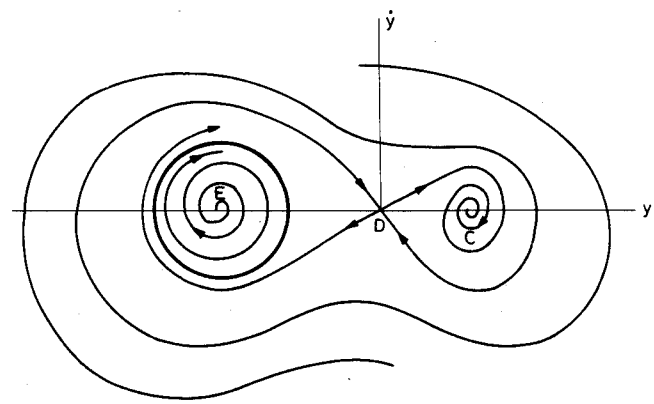

Fig. 10 Topological model for QSS solution.

stable and the resonance solution unstable—very desirable from the point of view of the missile designer. For some such values of $\bar{H}$, the roll response is likely to be similar to that in Fig. 8, but about a mean value of unity; the total incidence angle would build up, showing a divergent and unbounded behavior similar to Fig. 9. Thus, it is possible to demonstrate the phenomenon of catastrophic yaw without explicitly considering induced side forces and moments in the analysis.

Conclusions

Normal resonant lock-in is found to occur for a wide range of initial conditions, whereas reverse resonant lock-in is rarely observed. Two-dimensional topological models are built to bring out the dependence of steady lock-in on initial conditions. Quasisteady-state solutions can occur about an unstable equilibrium point. Thus, quasisteady lock-in at resonance is possible and unstable equilibrium solutions determined by Lyapunov's first method cannot be dismissed as of no engineering significance. The effect of nonlinear induced side forces and moments at resonance can be modeled by a decreased value of the yaw damping to show the unbounded yaw response of catastrophic yaw.

Acknowledgment

The authors wish to express their appreciation to C. H. Murphy and to the reviewers for their critical evaluations and suggestions.

References

[1]McShane, E. J., Kelley, J. L., and Reno, F. V., *Exterior Ballistics,* Univ. of Denver Press, Denver, CO, 1953.

[2]Chadwick, W. R., "Flight Dynamics of a Bomb with Cruciform Tail," *Journal of Spacecraft and Rockets,* Vol. 4, No. 6, 1967, pp. 768–773.

[3]Nicolaides, J. D., "A Review of Some Recent Progress in Understanding Catastrophic Yaw," AGARD Rept. 551, 1966.

[4]Price, D. A., Jr., "Sources, Mechanisms, and Control of Roll Resonance Phenomena for Sounding Rockets," *Journal of Spacecraft and Rockets,* Vol. 4, No. 11, 1967, pp. 1516–1525.

[5]Barbera, F. J., "An Analytical Technique for Studying the Anomalous Roll Behavior of Re-Entry Vehicles," *Journal of Spacecraft and Rockets,* Vol. 6, No. 11, 1969, pp. 1279–1284.

[6]Murphy, C. H., "Symmetric Missile Dynamic Instabilities," *Journal of Guidance and Control,* Vol. 4, No. 5, 1981, pp. 464–471.

[7]Murphy, C. H., "Some Special Cases of Spin-Yaw Lock-In," *Journal of Guidance, Control, and Dynamics,* Vol. 12, No. 6, 1989, pp. 771–776.

[8]Murphy, C. H., "Response of an Asymmetric Missile to Spin Varying Through Resonance," *AIAA Journal,* Vol. 9, No. 11, 1971, pp. 2197–2201.

[9]Ananthkrishnan, N., "Roll Resonance and Lock-In of Finned Projectiles," M.Tech. Thesis, Aerospace Engineering Dept., Indian Inst. of Technology, Kanpur, India, Nov. 1990.

Gerald T. Chrusciel
Associate Editor